Appl. Phys. B 49, 145–148 (1989)

Applied Physics B Photophysics and Laser Chemistry

Tunable UV Laser Photolysis of Organometallics with Product Detection by Laser Mass Spectroscopy: Trimethylaluminum

Th. Beuermann and M. Stuke

Max-Planck-Institut für biophysikalische Chemie, Postfach 2841,
D-3400 Göttingen, Fed. Rep. Germany

Received 21 December 1988/Accepted 9 March 1989

Abstract. We use tunable UV laser light in the region 200–320 nm, produced by frequency doubling the output of a dye laser, for the decomposition of organometallic compounds. This method has been applied to TMA, trimethylaluminum $Al(CH_3)_3$. Only the TMA monomer absorbs UV light for $\lambda > 220$ nm. TMA decomposes by one-photon absorption mainly into two channels: aluminum atoms Al plus organic fragments, and aluminummonomethyl $AlCH_3$ molecules plus organic fragments. The ratio $[Al]/[AlCH_3]$ is wavelength dependent. We present a mechanism to explain the photolysis of trimethyl compounds of group III elements (Al, Ga, In).

PACS: 81.15, 82.50

Organometallic compounds are widely used as a source of elements generated upon exposure to energy, which may be thermal or energetic beams in the form of photons [1–10], electrons [11, 12] or ions [13–16]. We describe an experiment, in which we use tunable UV laser photons of precisely defined energy for the decomposition of gaseous organometallics, namely $Al(CH_3)_3$. Our results show how organometallics of the trimethyl type (Al, Ga, In) interact with UV (laser) light.

1. Experimental Setup

A detailed description of the experimental setup can be found in [17]. A tunable UV laser light source photolyses the compound under investigation. Tunable UV output is generated by frequency doubling (SHG) the output of a XeCl excimer laser pumped dye laser in a β-barium-borate crystal (BBO). With this arrangement it is possible to tune the photolysis laser wavelength between 205 and 320 nm [18]. Moreover, one can cover the range 200–207 nm by sum frequency generation (SFG) [18]. Photolysis at 193 nm was performed by using an ArF excimer laser.

We use a weakly focussed KrF excimer laser ($\lambda = 248$ nm) to detect the photoproducts by nonresonant two-photon ionization similar to the detection of $GaCH_3$ as a photoproduct of trimethylgallium described earlier [8]. Alternatively, photoproducts can be detected by resonant multiphoton ionization (REMPI). Applying this technique, it was shown [6] that $AlCH_3$ is a photoproduct of TMA.

The data presented here were obtained by exposing TMA molecules (Alfa Ventron) in the ionization region of a laser time-of-flight mass spectrometer to the UV laser light source described above at a pressure of 10^{-4} Torr. Then, after a time delay of 200 ns, the neutral photoproducts were ionized by a KrF laser.

2. Results

2.1. Absorption Spectrum of TMA

We used a 1.5 m long cuvette with quartz windows and the frequency doubled dye laser as UV source to measure the absorption spectrum of TMA, which is shown in Fig. 1. The structureless spectrum in the far UV region points to a dissociative continuum of TMA. The cross section begins to rise at about 250 nm until

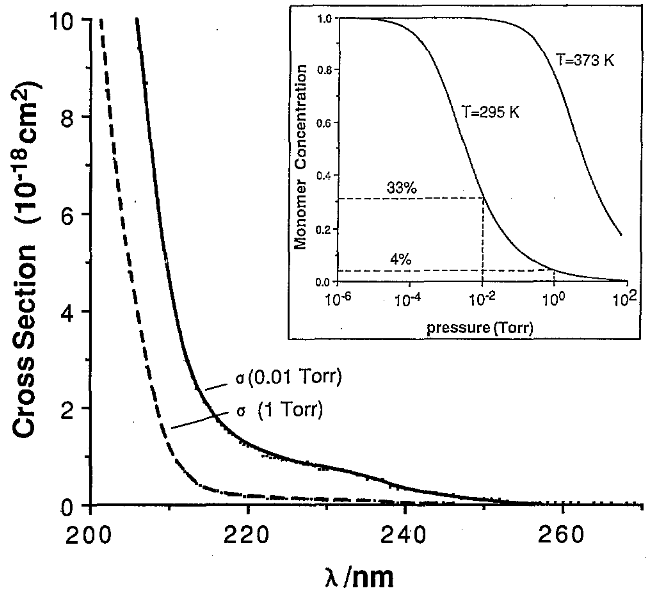

Fig. 1. UV absorption spectrum of TMA for a pressure of 0.01 Torr and 1 Torr, respectively. σ denotes the weighted average of σ(TMA monomer) and σ(TMA dimer). Insert: Pressure dependence of the monomer concentration in TMA for a temperature of 295 K and 373 K (the curves were calculated using the equilibrium constant given in [19])

220 nm, where a new channel seems to open. *The cross section is pressure dependent due to dimer formation.* For a given temperature, the monomer/dimer ratio strongly depends on the pressure (insert of Fig. 1) [19]. For example, at room temperature the monomer fraction in TMA amounts to only 4% at $p = 1$ Torr while is 33% at $p = 0.01$ Torr (see insert), i.e. by changing the pressure from 1 Torr to 0.01 Torr the monomer fraction is multiplied by a factor 8. *For $\lambda > 220$ nm only the monomer absorbs.* This can be seen from Fig. 2, where the ratio of the cross sections at $p = 0.01$ Torr and $p = 1$ Torr is plotted versus laser wavelength, showing an asymptotic approach to the predicted value $\sigma(0.01\ \text{Torr})/\sigma(1\ \text{Torr}) = 8$. Here σ denotes the weighted average of the individual σ's of the monomer and the dimer.

2.2. Photolysis of TMA

Typical time-of-flight mass spectra of TMA at $\lambda = 193$ nm (ArF) can be seen in Fig. 3. Ions generated by the photolysis laser alone (top trace) are Al$^+$ and Al(CH$_3$)$_2^+$. The detection laser (KrF) itself generates only a small amount of Al$^+$ (bottom trace). If the detection laser is triggered after a suitable delay of $\Delta t = 10.2$ µs with respect to the photolysis laser, the mass spectrum shown in the middle trace is obtained. In addition to the ions from the top trace, AlCH$_3^+$ and Al$^+$ ions are detected, due to the corresponding neutral species. Other photoproducts were not detected. The enhancement of the Al$^+$ and AlCH$_3^+$ peaks with respect to the background (bottom trace) is a measure for the relative amount of the corresponding neutral fragments produced by the photolysis laser. The above-mentioned enhancement divided by the number of photons per laser pulse gives the relative ion yield Y of a photoproduct. The Al$^+$ and AlCH$_3^+$ signals depend linearly upon the photolysis laser energy, a

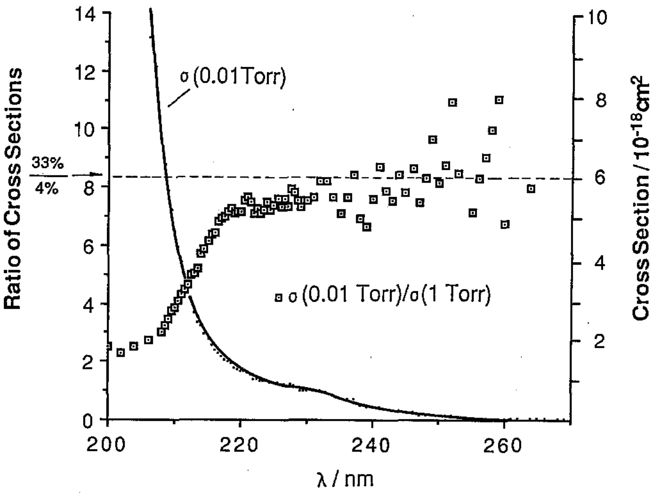

Fig. 2. Ratio of the UV absorption cross sections at 0.01 Torr and 1 Torr as a function of the wavelength. The cross section for 0.01 Torr is plotted for comparison

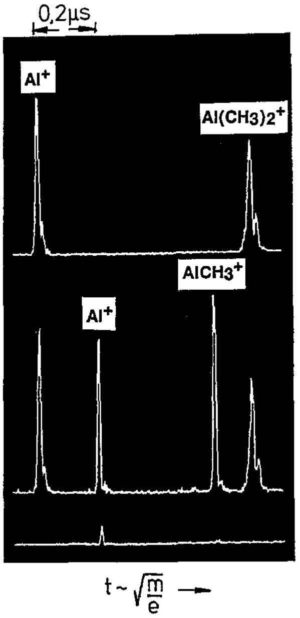

Fig. 3. Ion time-of-flight signal of trimethylaluminum $Al(CH_3)_3$, induced by the photolysis laser at 193 nm alone (top trace), and after ionization of neutral species, formed by the photolysis laser, by a weakly focussed KrF excimer laser (detection laser) delayed by 200 ns (middle trace). The control experiment, with the detection laser alone, is shown in the bottom trace (see text for details)

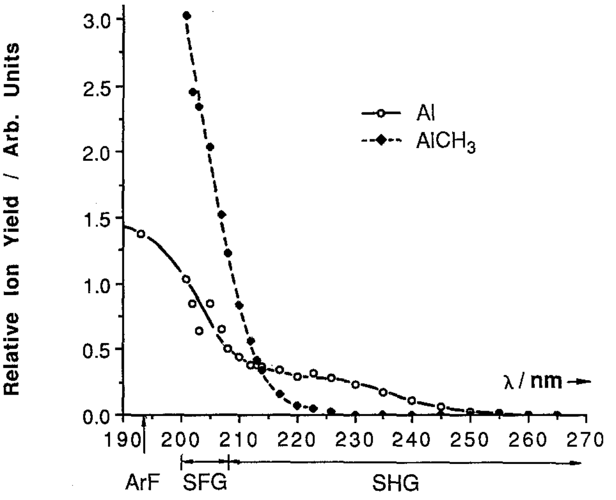

Fig. 4. Relative ion yields of Al and $AlCH_3$ as a function of the photolysis laser wavelength

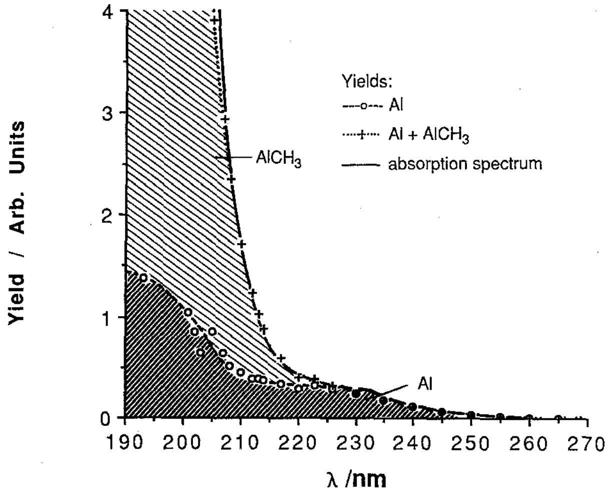

Fig. 5. The relative amounts of gaseous TMA decomposition products as a function of photolysis laser wavelength in comparison to the absorption spectrum

fact, which strongly suggests that TMA decomposes by a *one*-photon process. The obtained yields $Y(Al^+)$ and $Y(AlCH_3^+)$ are shown in Fig. 4 as a function of the photolysis laser wavelength. The threshold for Al production is at about 255 nm, whereas the $AlCH_3$ yield has its onset at 230 nm. For the case of resonant detection of the photoproducts Al and $AlCH_3$ described in [6], the photolysis laser wavelength dependence of the yields is the same [20].

3. Discussion

Since the two-photon ionization probabilities of Al and $AlCH_3$ are different, the relative ion yields must be calibrated in order to obtain the absolute yields Y(Al) and $Y(AlCH_3)$. The fact that only small amounts of $Al(CH_3)_2$ were detected [21], suggests a TMA decomposition mainly into the two channels Al plus organic fragments and $AlCH_3$ plus organic fragments. Assuming TMA to have a purely dissociative transition in the region under investigation (190–270 nm), the sum of both fragmentation channels $[Y(Al)+Y(AlCH_3)]$ should fit the absorption spectrum of TMA. Within our experimental accuracy this holds only for

$$Y(AlCH_3)/Y(Al) = 1.5\, Y(AlCH_3^+)/Y(Al^+),$$

with the factor 1.5 compensating for the different ionization probabilities of Al and $AlCH_3$ at 248 nm (Fig. 5).

The quantum yield is $\Phi_x := N_x/N$, where x stands for Al or $AlCH_3$, N_x is the number of photons in the x-channel and N is the total number of absorbed photons. From the proportionalities $Y_x \propto N_x$ and $A(\lambda) \propto N$, for an absorption coefficient A much smaller than 1, it follows that $\Phi_x \propto Y_x/A$.

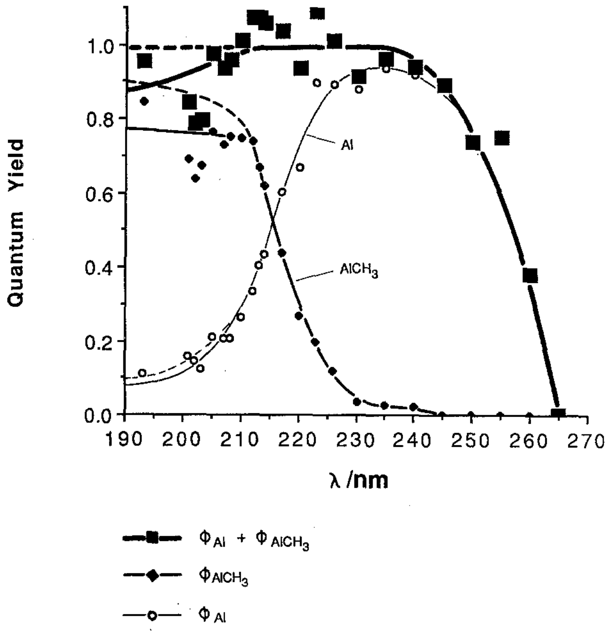

Fig. 6. Quantum yield Φ for the two fragmentation channels forming Al atoms and $AlCH_3$ molecules and the sum of both. The yields were calculated from $\Phi = Y/A$, where Y is the yield of a photoproduct and A the measured absorption coefficient of TMA at 0.01 Torr (see text for details)

In Fig. 6 we have plotted the relative quantum yields $F_x = Y_x/A$ against the wavelength of the photolysis laser. Obviously the quantum yield for Al production remains constant between 225 and 250 nm. This means, that the decomposition of TMA in this interval predominantly leads to aluminum atoms and organic fragments. Below 230 nm, the formation of $AlCH_3$ molecules becomes more and more important, but both quantum yields sum up to a constant all the way down to 210 nm. Below this value, the sum of both channels begins to decrease. A reason for this behaviour can be the uncertainty of the absorption spectrum for low pressures ($p < 0.001$ Torr). Nevertheless, only small amounts of other photoproducts were detected in this region, so that we are confident that the dashed lines in Fig. 6 reflect the real photochemistry of TMA.

4. Dissociation Mechanism of TMA

One striking feature of our results is that aluminum atoms are produced at lower photon energies than $AlCH_3$. Since the average bond energy of an Al–CH_3 bond in TMA is reported to be about 2.9 eV [22], one expects 8.7 eV to be necessary in order to separate all three CH_3 ligands. On the other hand our experiments show that one 5 eV photon is sufficient to isolate the Al atom. In order to explain the energy mismatch of 3.7 eV, we propose a mechanism which sets energy free:

$$\left.\begin{aligned} Al(CH_3)_3 + h\nu &\xrightarrow{h<255\ \mathrm{nm}} Al(CH_3)_2^{\dagger} + CH_3 \\ Al(CH_3)_2^{\dagger} &\longrightarrow Al + C_2H_6\,. \end{aligned}\right\} \qquad (1)$$

The formation of C_2H_6 (ethane) as a direct photoproduct seems to be the only explanation for our surprising experimental results. Due to the high ionization potential of ethane (11.6 eV), however, the collision free detection of C_2H_6 as a photoproduct is difficult with our present experimental setup.

The mechanism for the production of $AlCH_3$ is:

$$Al(CH_3)_3 + h\nu \xrightarrow{\lambda<230\ \mathrm{nm}} AlCH_3 + CH_3 + CH_3\,, \qquad (2)$$

without the gain of energy through the formation of a stable molecule like C_2H_6. If TMA were to decompose via

$$Al(CH_3)_3 + h\nu \rightarrow AlCH_3 + C_2H_6\,,$$

similar to the first mechanism (1), then $AlCH_3$ should appear at lower photon energies than the Al atom. This is not the case (compare Fig. 4–6). Taking the average binding energy of 2.9 eV, one would expect the threshold for the $AlCH_3$ production via the second process (2) at about 5.8 eV. Since for sequential removal of CH_3 the second Al–C bond in TMA is weaker than the first and third, due to unpairing of the two *s*-electrons in the aluminum atom [23], a red shift to a somewhat smaller value can be expected. This is in good agreement with the observed onset of the $AlCH_3$ yield at 5.4 eV (230 nm) (cf. Figs. 4–6).

Our results on TMG, trimethylgallium $Ga(CH_3)_3$, show that the wavelength dependence of the Ga and $GaCH_3$ yields is similar to the case of TMA [24]. Additionally, we detected neutral In atoms after the photolysis of TMI (trimethylindium) at 308 nm (4 eV), although at least 5.3 eV are necessary to break all three In–C bonds [22]. Therefore we conclude that TMA, TMG, and TMI all have the same dissociation mechanism.

5. Conclusion

We have shown that for gas phase TMA only the monomer absorbs UV light for $\lambda > 220$ nm. The decomposition of TMA by UV laser light is a one-photon process with Al and $AlCH_3$ as the main Al-containing photoproducts. The ratio $[AlCH_3]/[Al]$ is strongly wavelength dependent. This can be explained by the proposed dissociation mechanism given in (1) and (2).

Acknowledgements. We would like to acknowledge stimulating discussions with Y. Zhang, technical assistance by K. Müller and W. Sauermann, support by F. P. Schäfer, and financial support by SFB 93 („Photochemie mit Lasern“, C2+C15) and BMFT (Nr. 13N5398/7).

References

1. T.F. Deutsch, D.J. Ehrlich, R.M. Osgood, Jr.: Appl. Phys. Lett. **35**, 175 (1979)
2. D.J. Ehrlich, J.Y. Tsao: J. Vac. Sci. Technol. B **1**, 969 (1983)
3. G.S. Higashi, C.G. Fleming: Appl. Phys. Lett. **48**, 1051 (1986)
4. C. Jonah, P. Chandra, R. Bersohn: J. Chem. Phys. **55**, 1903 (1971)
5. Y. Zhang, M. Stuke: J. Cryst. Growth **93**, 143 (1988)
6. Y. Zhang, M. Stuke: Jap. J. Appl. Phys. **27**, L1349 (1988)
7. Y. Zhang, M. Stuke: Chem. Phys. Lett. **149**, 310 (1988)
8. Y. Zhang, Th. Beuermann, M. Stuke: Appl. Phys. B **48**, 97 (1989)
9. S.A. Mitchell, P.A. Hackett: J. Chem. Phys. **79**, 4815 (1983)
10. K. Ziegler, N.-R. Kroll, W. Larbig, O. Steudel: Ann. Chem. **629**, 53 (1960)
11. R.W. Bigelow, J.G. Black, C.B. Duke, W.R. Salaneck, H.R. Thomas: Thin Solid Films **94**, 233 (1982)
12. S. Okazaki: In Proceedings of the International Conference on Microlithography, Vienna 1988
13. K. Gamo, N. Takakura, N. Samoto, R. Shimizu, S. Namba: Jpn. J. Appl. Phys. **23**, L239 (1984)
14. G.M. Shedd, H. Lezec, A.D. Dubner, J. Melngailis: Appl. Phys. Lett. **49**, 1584 (1986)
15. W. Coburn, H.F. Winters, T.J. Chuang: J. Appl. Phys. **48**, 3532 (1977)
16. T.M. Mayer, R.A. Barker, L.J. Whitman: J. Vac. Sci. Technol. B **4**, 176 (1981)
17. R. Larciprete, M. Stuke: J. Phys. Chem. **90**, 4586 (1986)
18. P. Lokai, B. Burkhardt, D. Basting, W. Mückenheim: Laser und Optoelektronik **3**, 296 (1987)
19. C.H. Henrickson, D.P. Eyman: Inorg. Chem. **6**, 1461 (1967)
20. Th. Beuermann, M. Stuke: Unpublished results
21. Th. Beuermann, M. Stuke: To be published
22. G. Pilcher, H.A. Skinner: In *The Chemistry of the Metal-Carbon Bond*, ed. by F.R. Hartley, S. Patai (Wiley, New York 1982) Vol. 1, p. 69
23. W.A. Goddard III, L.B. Harding: Ann. Rev. Phys. Chem. **29**, 363 (1978)
24. Th. Beuermann, M. Stuke: To be published